Exchange Kinetics of Individual Amide Protons in ^{15}N-Labeled Helical Peptides Measured by Isotope-Edited NMR†

Carol A. Rohl and Robert L. Baldwin*

Department of Biochemistry, Stanford University School of Medicine, Stanford, California 94305

Received April 1, 1994; Revised Manuscript Received May 12, 1994®

ABSTRACT: Amide proton exchange measured by one-dimensional ^{15}N-edited proton NMR has been used to probe helical structure in an alanine-based peptide. This study is the first report of individual peptide NH exchange rates determined in a simple, repeating sequence peptide whose helical structure can be predicted by helix-coil theory. Measured protection factors directly demonstrate that the ends of the helix are frayed. The protection factors are compared to the Lifson–Roig theory, modified to include N-capping, using known values for helix propensities and N-cap propensities. Base-catalyzed exchange rates are shown to measure the extent of hydrogen bonding of the peptide NHs, and the results are fitted by a simple model in which hydrogen bonding of the peptide NH group provides protection and no exchange occurs from the hydrogen-bonded state. Protection from acid-catalyzed exchange correlates with hydrogen bonding by both the NH and CO groups of a peptide unit: the data are fitted by a model in which exchange occurs only when both hydrogen bonds formed by a peptide unit are broken. This result indicates that acid-catalyzed exchange occurs by the O-protonation mechanism, in agreement with earlier work [Perrin & Arrhenius (1982) *J. Am. Chem. Soc. 104,* 6693–6696; Perrin et al. (1984) *J. Am. Chem. Soc. 106,* 2749–2753; Tüchsen & Woodward (1985) *J. Mol. Biol. 185,* 421–430].

Linderstrøm-Lang (1955) proposed that amide proton exchange could be used to characterize hydrogen-bonded secondary structures in proteins. In agreement with this proposal, protection from exchange has been found to be correlated with hydrogen-bonded secondary structure; nearly all strongly protected amides in proteins are found in α-helices and β-sheets (Wagner & Wüthrich, 1982; Englander & Kallenbach, 1984; Woodward et al., 1982). Site-specific measurements of exchange rates have been made for helical segments in proteins and naturally occurring peptides including the S-peptide moiety of RNase S (Kuwajima & Baldwin, 1983), the N-terminal helix of cytochrome *c* (Wand et al., 1986), and the bee venom apamin which contains a C-terminal α-helix (Dempsey, 1986). Wild-type melittin, a helix-forming peptide, and a helix-stabilizing mutant (Pro→Ala) have also been characterized by amide proton exchange in methanol (Dempsey, 1988, 1992). Zhou et al. (1994) measured amide exchange rates in a short, stable α-helix prenucleated by a side chain to side chain lactam bridge. These studies support the correlation observed between protection from exchange and the formation of helical hydrogen bonds. Analysis of exchange kinetics in these systems by helix-coil transition theory, however, is not straightforward. Side chain–side chain interactions and tertiary interactions contribute to the stability of these helices and affect observed protection factors. Electrostatic interactions cause pH-dependent changes in stability and interfere with the measurement of the acid- and base-catalyzed exchange rates from the pH dependence of exchange.

Exchange rates measured in a simple system should aid in understanding the mechanisms of protection in proteins. An isolated peptide helix of uniform sequence provides a simple system for which rigorous interpretation of the observed exchange kinetics is possible in terms of well-established helix-coil theories that have been used successfully to interpret data from helical peptides (Scholtz et al., 1991a; Rohl et al., 1992; Gans et al., 1992; Scholtz et al., 1993; Chakrabartty et al., 1994). The factors that contribute to helical stability in isolated peptides are beginning to be well characterized [reviewed by Scholtz and Baldwin (1992) and Chakrabartty and Baldwin (1994)], making it possible to design helical peptides that contain chiefly one amino acid and are devoid of side chain interactions. Alanine-based peptides that contain occasional lysine residues to ensure solubility in water fulfill these requirements (Marqusee et al., 1989). Exchange kinetics are measured in the pH range 1–5 in order to obtain both acid- and base-catalyzed rates, and the helical stability of these peptides is independent of pH in this range. Here we utilize ^{15}N-labeled synthetic peptides to measure site-specific amide exchange rates in a 21-residue alanine-based peptide helix. The acid- and base-catalyzed exchange rates are interpreted primarily in terms of hydrogen bonding in the helix. We find that protection from base-catalyzed exchange measures directly the extent of hyrdrogen bonding of a peptide NH. Protection from acid-catalyzed exchange is more complex and can be correlated with hydrogen bonding of both the NH and CO groups of a given peptide unit. This finding supports the O-protonation mechanism for acid-catalyzed exchange. The measured protection factors are interpreted quantitatively in terms of helix-coil theory.

EXPERIMENTAL PROCEDURES

Peptide Synthesis and Purification. Peptides were synthesized by stepwise solid-phase procedures using pentafluorophenyl esters of fluorenylmethyloxycarbonyl (Fmoc) amino acids (Atherton & Sheppard, 1989). Fmoc-[^{15}N]alanine was prepared from [^{15}N]alanine (>99 atom %, Cambridge Isotope Labs) as described by Stewart and Young (1984). The labeled residues were coupled onto the peptides using the 1-hydroxybenzotriazole/benzotriazol-1-yloxy-tris(dimethylamino)phosphonium hexafluorophosphate (HOBt/BOP) method (Hud-

† This work was supported by a grant from the National Science Foundation (MCB 920-8648).

* To whom correspondence should be addressed.

® Abstract published in *Advance ACS Abstracts,* June 15, 1994.

0006-2960/94/0433-7760$04.50/0

son, 1988). The crude peptides were purified by reverse-phase FPLC[1] with gradients of acetonitrile containing 0.1% trifluoroacetic acid. Peptide purity was greater than 95% as shown by reverse phase FPLC. Molecular weights were determined by FAB or electrospray mass spectrometry.

NMR Spectroscopy. Samples were prepared by dissolving peptide in water to a concentration of 1–2 mM, adjusting the pH to the desired value with hydrochloric acid, and then lyophilizing to dryness. To initiate exchange, the peptide was dissolved at 1–2 mM in ^2H_2O at 5 °C containing 1 M sodium chloride and 5 mM sodium phosphate at the desired final pH*. pH* represents the glass-electrode reading at room temperature, uncorrected for isotope effects. All reported pH* measurements were made after the acquisition of the NMR spectra. After the peptide was dissolved in buffer, multiple spin echo difference spectra (Freeman et al., 1981; Bendall et al., 1981) were acquired throughout the exchange on a General Electric GN-Omega spectrometer operating at a ^1H frequency of 500.13 MHz and ^{15}N frequency of 50.68 MHz. Nitrogen decoupling was accomplished using the WALTZ-16 decoupling scheme (Shaka et al., 1983). Data were collected using a 5000-Hz spectral width. The FID was the sum of 64 scans collected in 4096 complex points with an acquisition time of 0.82 s and a 5-ms recycle delay. Spectra were processed using the FELIX software package (release 2.1, Biosym Inc.) on a Silicon Graphics Indigo computer. FIDs were multiplied by an exponential decay function with line broadening of 3 Hz prior to Fourier transformation. Exchange rate constants were determined by least-squares analysis of the peak intensities fitted to a single-exponential decay.

Data Analysis. The pH dependences of individual amides were fitted to the rate equation describing exchange:

$$k_{obs} = k_H 10^{(-pH)} + k_{OH} 10^{(pH-pK_w)} \quad (1)$$

where k_H and k_{OH} are the rate constants for the acid- and base-catalyzed mechanisms, respectively, and $pK_w = 15.653$ for ^2H_2O at 5 °C (Covington et al., 1966). This equation assumes that water-catalyzed exchange is negligible (Gregory et al., 1983) and that acid- and base-catalyzed exchange are both first order in catalyst concentration. Equation 1 can be rewritten as described previously (Robertson & Baldwin, 1991; Roder et al., 1985):

$$k_{obs} = (k_{min}/2)[10^{(pH-pH_{min})} + 10^{(pH_{min}-pH)}] \quad (2)$$

where k_{min} and pH_{min} are the exchange rate constant and pH, respectively, at the point of slowest exchange. pH_{min} is related to the acid- and base-catalyzed rate constants by the expression

$$pH_{min} = [pK_w + \log(k_H/k_{OH})]/2 \quad (3)$$

Equation 1 was fitted to rate constant data for individual amide protons in both the helical and the nonhelical reference peptides using the modified Gauss–Newton nonlinear function minimization program NONLIN (Michael Johnson) on a Silicon Graphics Personal Iris. Observed rate constants were weighted by the reciprocal of their magnitude so as not to favor points far from the pH_{min} (Robertson & Baldwin, 1991). Confidence intervals were evaluated at 65%. Protection factors were calculated as the ratio of exchange rate constants determined for amide protons in the nonhelical reference peptide to those determined for amides in the helical peptide. Reported pH_{min} values were determined from eq 3.

Application of Lifson–Roig Theory. The Lifson–Roig statistical mechanical model for the helix-coil transition (Lifson & Roig, 1961) describes the helix content of a peptide in terms of the chain length, n, and a propagation parameter, w, and nucleation parameter, v, for each component residue. The chain length, n, is the number of residues that are flanked on both sides by peptide bonds. In a blocked peptide with n amino acids, there are $n+1$ peptide units and each amino acid is a residue. According to this numbering scheme, peptide unit i is immediately N-terminal to residue i. The statistical weights w and v are assigned to residues that are constrained to a helical conformation as defined by their (ϕ,ψ) angles. Nucleating and propagating helical residues are distinguished by considering the conformation of the adjacent residues; nucleating residues have at least one coil neighbor. The N-terminal acetyl and C-terminal carboxamide blocking groups cannot be constrained to helical (ϕ,ψ) space and, therefore, are by definition in the coil conformation. The original Lifson–Roig model has been modified to include N-capping interactions described by the parameter *n-value* (Doig et al., 1994). The N-cap parameter describes the preference of a particular residue, relative to alanine, to be in a coil conformation with a helical N-terminal neighbor. The complete partition function for the helix-coil transition is calculated from eq 5 of Doig et al. (1994).

According to the Lifson–Roig formalism, residue i is considered to be a stabilized helical residue that contributes statistical weight w to the partition function only when residues $i-1$, i, and $i+1$ are in the helical conformation as defined by their (ϕ,ψ) angles. This condition is necessary and sufficient for formation of the hydrogen bond between the NH of peptide unit $i-2$ and the CO of peptide unit $i+1$ (Lifson & Roig, 1961). The probability of an individual hydrogen bond forming, therefore, can be recursively related to stabilized helix probability:

$$f_B^{NH}(i) = f_H(i-2) \quad (4)$$

$$f_B^{CO}(i) = f_H(i+1) \quad (5)$$

$f_B^{NH}(i)$ and $f_B^{CO}(i)$ refer to the probability of formation of the NH and CO hydrogen bond, respectively, of peptide group i. $f_H(i)$ refers to the probability that residue i is a stabilized helical residue and can be calculated directly from the helix-coil partition function as previously described (Doig et al., 1994). The helix propagation and N-cap parameters have been determined independently using CD to measure the total helix content of a large number of alanine-based peptides that have various substitutions at different positions (Chakrabartty et al., 1994). The values used in the partition function calculation here are w(Ala) = 1.61, w(Lys) = 0.82, *n-value*(Ala) = 1.0, *n-value*(Lys) = 0.4, and *n-value*(acetyl) = 9.7. The free energy of helix initiation is a property of the helix backbone and appears to be relatively independent of side chain identity (Ptitsyn, 1972; Scholtz et al., 1991a; Rohl et al., 1992). The initiation parameter used here for all residues, $v = 0.048$, was determined previously (Rohl et al., 1992).

RESULTS

Peptide and Experimental Design. The 21-residue peptide Ac-$(AAKAA)_4$Y-NH_2 is a well-behaved peptide helix (Rohl

[1] Abbreviations: FPLC, fast protein liquid chromatography; FAB, fast atom bombardment; NMR, nuclear magnetic resonance; CD, circular dichroism; FID, free induction decay; NOE, nuclear Overhauser effect; BPTI, bovine pancreatic trypsin inhibitor.

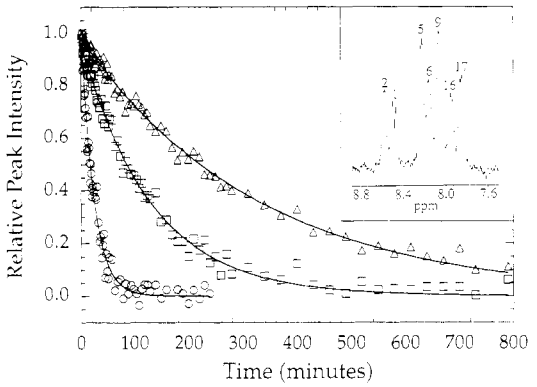

FIGURE 1: Representative exchange data for amide protons in the 21-residue peptide. The inset shows an ^{15}N-edited ^{1}H NMR spectrum of the 21-residue peptide with [^{15}N]alanine incorporated at positions 1, 2, 5, 6, 9, 16, and 17. The spectrum was acquired 3.3 min after the initiation of exchange at pH* 3.60. The amide proton resonance of alanine 1 is not completely decoupled and shows residual ^{15}N–H coupling. The main panel shows kinetic curves for three of the amide protons from the spectrum in the inset. Data are for the amide protons of residue (○) 1, (□) 5, and (△) 9. Lines are the best fit of a single-exponential decay to the data.

et al., 1992) with mean residue ellipticity at 222 nm of −27 500 deg cm^2 dmol^{-1} at 5 °C in 1 M sodium chloride and 5 mM sodium phosphate (data not shown). The high helix content of this peptide can be attributed predominantly to the strong helix propensity of alanine (Marqusee et al., 1989). The six-residue peptide Ac-AAKAAY-NH_2 shows no helical structure by CD (Rohl et al., 1992) and is used as a reference for the nonhelical state. These peptides have no titratable groups with pK_a values in the range from pH 1 to 5, and their helical stability is, therefore, expected to be independent of pH in the range where exchange measurements are made. This pH independence of stability has been demonstrated for peptides with highly related sequences (Marqusee et al., 1989). Both the helical and the nonhelical peptides have poor chemical shift dispersion in the amide region of the NMR spectrum, resulting from the sequence degeneracy. To overcome this problem, and to aid in assignment of individual amide protons, a series of peptides was made with [^{15}N]alanine substituted for alanine at specific sites in individual peptides. Initially, 16 helical and 4 nonhelical peptides were synthesized with single ^{15}N substitutions in order to obtain complete assignments of the alanine amide proton resonances by isotope-edited methods. Two additional helical peptides were then synthesized with multiple [^{15}N]alanine substitutions at sites designed to defeat the overlap problem. Representative exchange data, collected at pH* 3.60 for one peptide with [^{15}N]alanine incorporated at seven positions (residues 1, 2, 5, 6, 9, 16, and 17), are shown in Figure 1. The second peptide contained eight [^{15}N]alanine substitutions at positions 1, 2, 4, 10, 12, 14, 19, and 20. Exchange data were collected from both singly- and multiply-labeled peptides. A high ionic strength (1 M sodium chloride) was used to decrease the contribution of electrostatic interactions to the observed exchange kinetics.

pH-Dependent Exchange Behavior. The pH dependence of the observed exchange rate constant, k_{obs}, was measured for every alanine amide proton in both the helical and the nonhelical peptides. Acid- and base-catalyzed exchange rate constants, fitted from eq 1, and pH_{min} values, calculated from eq 3, are given in Table 1. In the nonhelical peptide, there are four amide protons that have an alanine side chain as their nearest C-terminal neighbor. These protons, however, have different N-terminal neighbors: either alanine, lysine, or the acetyl blocking group. Amide protons from these three different types of dipeptides are expected to have different pH_{min} and k_{min} values resulting from inductive effects (Molday et al., 1972) and steric hindrance (Bai et al., 1993) from the neighboring side chains. The solid symbols in Figure 2 show the pH dependences of the amide protons in the nonhelical peptide. Solid lines are the best fit of eq 1 to the data. The two amide protons with alanine N-terminal neighbors have the same pH dependence, within error, and data from both these amide protons have been fitted simultaneously.

Representative pH dependences for amide protons in the helical peptide are shown by the open symbols in Figure 2. Dashed lines are the best fits of eq 1 to these data. In each panel, the measured pH dependence for a single amide proton in the helical peptide is compared to the measured pH dependence of the nonhelical amide proton(s) with the same

Table 1: Amide Proton Exchange Parameters

peptide unit	dipeptide	k_H[a] (min^{-1})	k_{OH}[a] (10^{10} min^{-1})	pH_{min}[b]	ΔpH_{min}[c]	PF_H[d]	PF_{OH}[d]
Ac-AAKAAY-NH_2 (reference)							
1	Ac-A	280	1.2	4.01			
2, 5[e]	A-A	14	3.5	3.13			
4	K-A	608	3.0	3.00			
Ac-(AAKAA)$_4$Y-NH_2 (helix)							
1	Ac-A	80	1.8	3.65	−0.36	3.5	0.7
2	A-A	3.7	8.3	2.65	−0.48	3.8	0.42
4	K-A	0.98	1.1	2.80	−0.20	6.9	2.7
5	A-A	1.3	0.79	2.93	−0.20	10.8	4.4
6	A-A	1.1	0.66	2.94	−0.19	12.7	5.3
7	A-A	1.1	0.31	3.10	−0.03	12.7	11.3
9	K-A	0.46	0.34	2.89	−0.11	14.8	8.8
10	A-A	0.90	0.31	3.06	−0.07	15.5	11.3
11	A-A	0.79	0.25	3.08	−0.05	17.7	14.0
12	A-A	1.0	0.21	3.17	0.04	14.0	16.7
14	K-A	0.68	0.29	3.01	0.01	10.0	10.3
15	A-A	1.5	0.32	3.16	0.03	9.3	10.9
16	A-A	1.8	0.31	3.21	0.08	7.8	11.3
17	A-A	3.2	0.45	3.25	0.12	4.4	7.8
19	K-A	2.5	1.1	3.00	0.00	2.7	2.7
20	A-A	6.2	1.3	3.17	0.04	2.3	2.7

[a] Fitted from eq 1. Standard deviation ranges from 10 to 20% of the reported value. [b] Calculated from eq 3. Standard deviation ranges from 0.05 to 0.13 pH unit. [c] Relative to pH_{min} values for reference amide protons from the same dipeptide type. [d] Relative to rate constants for reference amide protons from the same dipeptide type. [e] Data for these protons were fitted simultaneously.

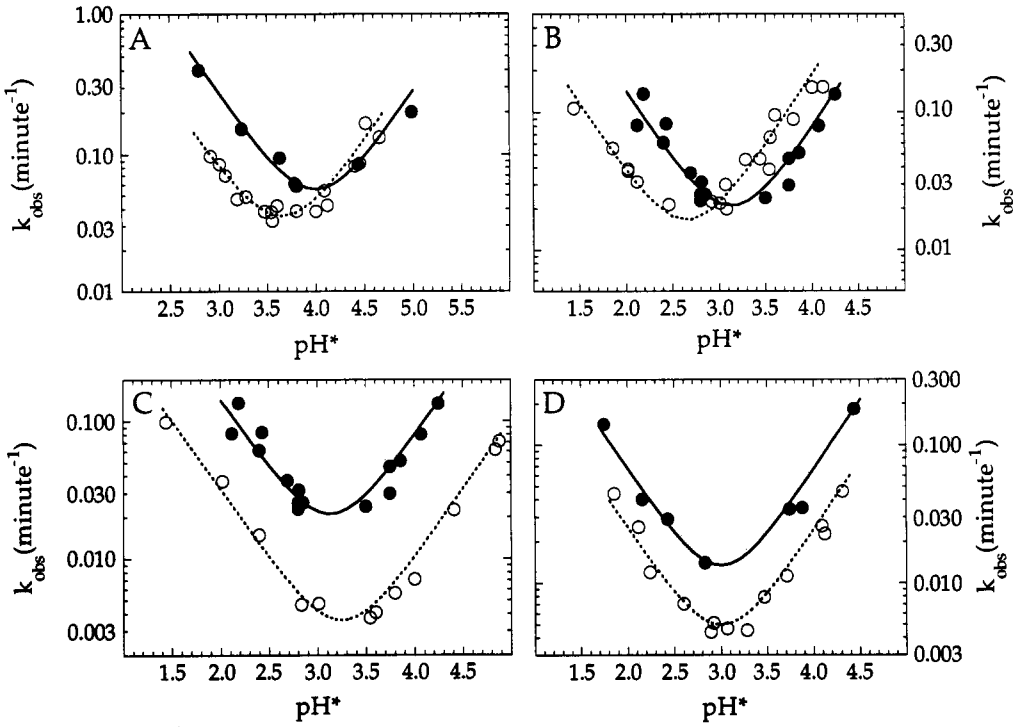

FIGURE 2: Representative pH dependences of observed exchange rates for amide protons in the helical and nonhelical peptides. Solid symbols (●) are data for amide protons from the nonhelical reference peptide. Measured rate constants are for amide protons from (A) the Ac-A dipeptide (position 1), (B) A-A dipeptides (positions 2 and 5), and (D) the K-A dipeptide (position 4). Solid symbols in panel C are identical to those in panel B. Open symbols (○) are data for amide protons from the helical peptide. Data for amide protons from residues (A) 1, (B) 2, (C) 17, and (D) 19 are shown. Each panel compares amide protons from the helical and nonhelical peptides that have the same nearest neighbors. Lines are the best fit of eq 1 to the data.

nearest neighbors. The measured pH_{min} values for amide protons in the helical peptide are shifted relative to reference pH_{min} values in the nonhelical peptide. The change in pH_{min} for all the helical amide protons, relative to the corresponding nonhelical reference amide protons, is given in Table 1. ΔpH_{min} shows a position dependence, with amides near the N-terminus having pH_{min} values shifted to significantly lower pH* and C-terminal amides having pH_{min} values shifted to slightly higher pH*.

The helical and nonhelical reference amide protons have the same nearest neighbors and their exchange rates have been measured under the same conditions. The observed shift in pH_{min} must result from the helical structure formed by the longer peptide. In general, anything that differentially affects the two mechanisms of exchange, acid- and base-catalyzed, will cause pH_{min} to change. To understand the effect helix formation has on pH_{min}, protection factors under conditions of acid- and base-catalyzed exchange must be considered independently. Protection factors for base-catalyzed exchange are shown as a function of position in Figure 3A. The experimentally determined protection factors reflect the pattern of NH hydrogen bonds in the peptide helix. The amide protons of residues 1 and 2, which cannot form helical hydrogen bonds, are not protected from exchange and actually exchange slightly faster than the reference nonhelical amide protons (see Discussion). All other peptide NHs, which can form helical hydrogen bonds, show varying degrees of protection with the exchange rates of the central amide protons being slowed by a factor of approximately 14–17 (Table 1). Protection factors for acid-catalyzed exchange (Figure 3B) do not show this simple correlation with the NH hydrogen-bonding pattern of the helix. The central amide protons are substantially protected from exchange (15–18-fold), and the protection factors again decrease toward the ends of the peptide (Table 1). Under conditions of acid-catalyzed exchange, however, there is still measurable protection (2–3-fold) at both termini of the peptide helix.

Application of the Lifson–Roig Model. The pH dependences for all amide protons in both peptides are well fitted by eq 1, indicating that exchange from the helix is occurring by the acid- and base-catalyzed EX2 mechanism (Hvidt, 1964). In this mechanism, a rapid equilibrium between open and closed states is followed by a relatively slow chemical exchange step. Although no exchange occurs from the closed state, amide protons exchange freely with solvent protons in the open state. The observed rate of exchange is the product of the intrinsic exchange rate and the probability of the open, exchange-competent state. The protection factor, which is defined simply as the ratio of the reference exchange rate to the rate in the presence of structure, is the reciprocal of the probability of the open state. For base-catalyzed exchange, conformations in which the amide group of peptide unit i is hydrogen bonded are considered to be incapable of exchanging. When this hydrogen bond is broken, exchange occurs freely. The protection factor of residue i, $PF_{OH}(i)$, can be calculated from

$$PF_{OH}(i) = 1/[1 - f_B^{NH}(i)] \quad (6)$$

where $f_B^{NH}(i)$, the probability that the NH of peptide unit i is hydrogen bonded, is determined from eq 4. Calculated protection factors for base-catalyzed exchange are shown by the solid line in Figure 3A.

Under conditions of acid-catalyzed exchange, the two N-terminal amide protons of the helical peptide show significant protection from exchange (Figure 3B). Since these peptide NHs cannot form helical hydrogen bonds, the simple correlation between protection and hydrogen bond formation by amide protons does not hold for the acid-catalyzed exchange reaction. The CO groups of these N-terminal peptide units,

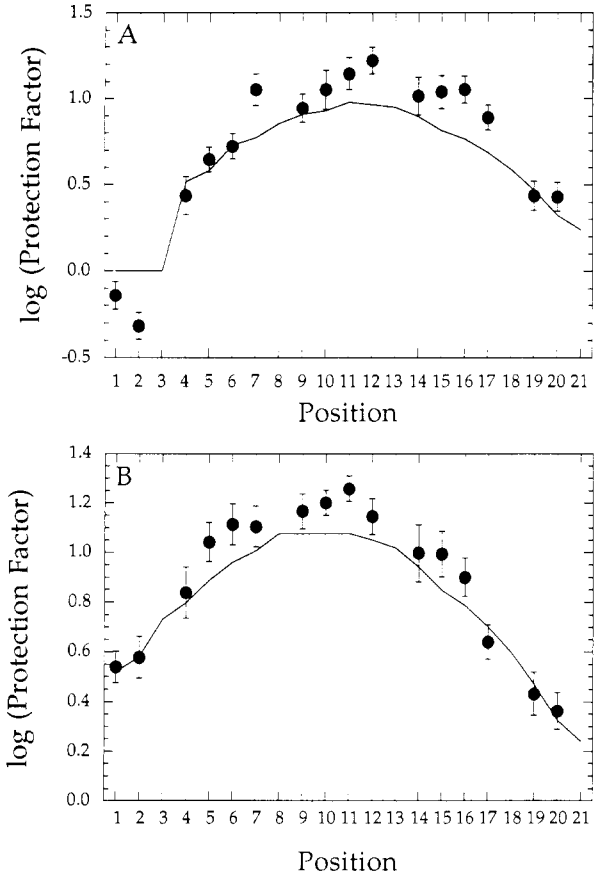

FIGURE 3: Position dependence of measured protection factors. Each protection factor is calculated as the ratio of the exchange rate constant for a helical amide proton to the exchange rate constant for the reference nonhelical amide proton with the same nearest neighbors. Error bars represent 65% confidence intervals. The solid lines are the predicted values of the protection factor (see text). (A) Protection from base-catalyzed exchange. (B) Protection from acid-catalyzed exchange.

however, can form helical hydrogen bonds. Similarly, the two C-terminal alanine amide protons also show significant protection from exchange. In these peptide units, the CO groups cannot form helical hydrogen bonds but the NH groups can. These observations suggest that protection of an amide proton from acid-catalyzed exchange results from hydrogen bond formation by either the NH or the CO group of a peptide unit (see Discussion). The model used to calculate protection factors for acid-catalyzed exchange, therefore, assumes that exchange cannot occur when either the NH or the CO of a peptide unit is hydrogen bonded; both hydrogen bonds must be broken for exchange to occur. Since the helix-coil transition is cooperative, with formation of a single hydrogen bond increasing the probability that a second hydrogen bond is formed, the probability that both the NH and CO hydrogen bonds are broken for a given peptide unit cannot be determined from a simple combination of eqs 4 and 5. Instead, the frequency of the exchanging conformation must be determined directly from the partition function by considering the statistical weights of residues $i+1$ and $i-2$ simultaneously. This treatment results in the calculated protection factors for acid-catalyzed exchange, PF_H, shown by the solid line in Figure 3B.

DISCUSSION

Fraying in Helical Peptides. Although the transition between α-helix and random coil in peptides is cooperative, it is not a two-state transition. Statistical mechanical models of the helix-coil transition predict that the ends of peptide helices will be frayed (Zimm & Bragg, 1959; Lifson & Roig, 1961). Helix fraying in peptides has been inferred from CD measurements of helix stability as a function of the position of an Ala→Gly substitution (Chakrabartty et al., 1991) and in NMR studies that have measured NOEs, CαH chemical shifts, or coupling constants (Jimenez et al., 1992; Liff et al., 1991; Bradley et al., 1990; Pease et al., 1990; Osterhout et al., 1989). Electron spin resonance spectroscopy of spin-labeled alanine-based helical peptides suggests that the helix termini are more mobile than the central regions of the helix (Miick et al., 1991, 1993). Total NH exchange measurements for helical polypeptides (Nakanishi et al., 1972) and peptides (Rohl et al., 1992) are consistent with helix fraying, but the observed kinetics are complex. Measurements of site-specific amide proton exchange rates for helical segments of proteins and naturally occurring peptides also provide some evidence for helix fraying, although the different helix propensities of the various amino acids probably contribute strongly to nonuniform stability in these helices (Wand et al., 1986; Dempsey, 1986, 1988, 1992). Poor dispersion of amide resonances has precluded the site-specific measurement of amide exchange rates by NMR in helical peptides of uniform sequence. By introducing ^{15}N-labeled residues into the peptide at specific sites and using standard heteronuclear NMR methods to obtain ^{15}N-edited proton NMR spectra, we are able to measure the exchange kinetics of individual amide protons in a simple alanine-based peptide helix. The measured exchange rates are slowest for amide protons in the center of the peptide and increase toward both termini, directly demonstrating that the ends of the helix are frayed.

Electron spin resonance studies of 16-residue helical peptides containing two spin labels have suggested that the ends of short alanine-based helices may exist in a 3_{10}- rather than α-helical conformation (Miick et al., 1992). Similar measurements made for a 21-residue peptide indicated that it adopted an α-helical conformation (Fiori et al., 1993). The α- and 3_{10}-helical conformations are distinguished by their hydrogen bonding patterns. In an acetyl-blocked peptide in which the acetyl group forms a helical hydrogen bond, the NH of the third peptide unit will form a helical hydrogen bond in a 3_{10}- but not in an α-helix. Amide exchange kinetics, therefore, should distinguish between the two conformations based on whether or not this amide proton is protected from base-catalyzed exchange. In the helical peptide studied here, the third residue is a lysine, and the exchange kinetics were not measured for the lysine amide protons. At the C-terminus, the CO group of peptide unit 19 should form a helical hydrogen bond to the carboxamide blocking group in 3_{10}- but not in α-helical conformation. Hydrogen bonding of the CO group would result in greater protection from acid-catalyzed exchange than from base-catalyzed exchange (see below). This amide proton, however, shows equal protection from acid- and base-catalyzed exchange, indicating that the C-terminus of this peptide is in an α-helical conformation.

Radford et al. (1992) noted that the folding kinetics of hen lysozyme measured by far UV CD do not coincide with the appearance of stably protected amide protons. The CD measurements indicate that more secondary structure is formed in the first several milliseconds of folding than is detected by amide exchange protection. Our measurements provide a possible explanation for this seeming discrepancy. Since CD reports on the extent of helix formation but amide exchange monitors the stability of helices, marginally stable helices may show significant ellipticity but only small

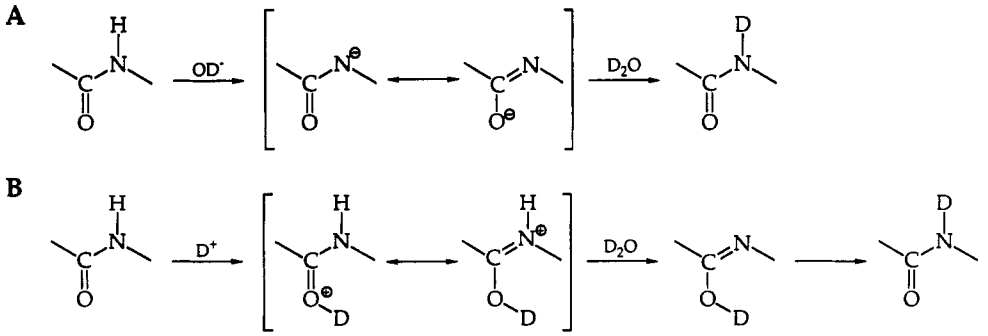

FIGURE 4: Chemical mechanism of the amide proton exchange reaction. (A) Base-catalyzed exchange occurs by direct abstraction of a proton from the peptide nitrogen. (B) Acid-catalyzed exchange occurs by protonation of the peptide carbonyl oxygen and involves an imidic acid intermediate.

protection factors. The 21-residue peptide studied here shows approximately 81% of the ellipticity expected for a fully helical peptide, but the measured protection factors are relatively small, reaching a maximum of 15–18 in the center of the peptide. The CD results are in reasonable agreement with the amide exchange measurements when both are compared by the modified Lifson–Roig theory. A mean helix content of 79% and maximal protection factors of about 12 are predicted independently by the modified Lifson–Roig theory using the known values of the helix and N-cap propensities of the component amino acids.

O-Protonation Affects ΔpH_{min}. The pH dependence of the amide exchange reaction reflects the fact that the chemical exchange step is both acid- and base-catalyzed. The base-catalyzed reaction occurs by direct abstraction of the proton from the peptide nitrogen by hydroxide (Figure 4A). Acid-catalyzed exchange occurs by protonation of the carbonyl oxygen, followed by deprotonation of the amide nitrogen by water, resulting in an imidic acid intermediate (Perrin & Arrhenius, 1982; Perrin et al., 1984). To complete the exchange reaction, these steps are then reversed (Figure 4B). Solvent accessibility and hydrogen bonding of the peptide NH affect both acid- and base-catalyzed exchange, since both mechanisms involve removal of the amide proton. Acid-catalyzed exchange, however, also involves proton transfer at the peptide CO. Perrin (1989) noted that the formation of the imidic acid intermediate in the acid-catalyzed exchange reaction reverses the hydrogen-bond donor-acceptor properties of the peptide. Consequently, he concluded that both the peptide oxygen and nitrogen must be dislodged from their hydrogen-bonded conformations for exchange to occur. Tüchsen and Woodward (1985) demonstrated that acid-catalyzed exchange rates, measured for the 25 most rapidly exchanging amide protons in BPTI, are correlated with the calculated solvent accessibilities of the peptide COs. The pH_{min} values for these protons varied widely, and the variations were attributed in part to an O-protonation step in the acid-catalyzed exchange reaction.

In the peptide helix, peptide NH hydrogen bonding provides protection from base-catalyzed exchange. The two N-terminal NHs, which cannot form helical hydrogen bonds, are not protected from exchange, while all other alanine amides show varying degrees of protection. Under acid-catalyzed exchange conditions, this simple relationship is not observed. Instead, protection is observed for all peptide NHs (Figure 3B). Hydrogen bonding of *either* the CO or the NH of a given peptide group is sufficient to provide protection from acid-catalyzed exchange, strongly supporting the O-protonation mechanism. Since two hydrogen bonds must be broken for acid-catalyzed exchange to occur but only one must be broken for base-catalyzed exchange to occur, slightly larger protection factors are observed for acid-catalyzed exchange than for base-catalyzed exchange. Consequently, the pH_{min} values of the helical amide protons should be decreased relative to nonhelical reference amide protons. The two most N-terminal NH protons cannot be protected from base-catalyzed exchange but are significantly protected from acid-catalyzed exchange, resulting in large decreases in pH_{min}. For the two most C-terminal alanine peptide units, whose CO groups cannot form helical hydrogen bonds, protection from both acid- and base-catalyzed exchange results exclusively from the NH hydrogen bond. In this case, there is equal protection against acid- and base-catalyzed exchange, and no change in pH_{min} is expected. These predictions are in reasonable agreement with our experimental results.

N-Terminal Amide Protons Show Enhanced Rates of Base-Catalyzed Exchange in the Helix. Although the hydrogen-bond network of the helix is sufficient to account for most of the observed exchange kinetics, the base-catalyzed exchange rates for the two most N-terminal amide protons cannot be explained by hydrogen bond formation. These amide protons cannot form helical hydrogen bonds, and the measured rates are actually faster than those determined for reference nonhelical amide protons (Table 1). This observed enhancement of the base-catalyzed exchange rate may result from the positive electrostatic potential at the N-terminal end of the helix macrodipole. Since the H^+ and OH^- ions that produce acid- and base-catalyzed exchange are charged, the local electrostatic potential of the helix macrodipole is expected to affect the rate of both exchange reactions. The distribution of pH_{min} values measured in methanol for amide protons of melittin and a helix-stabilizing mutant was consistent with the expected effects of the helix macrodipole (Dempsey, 1988, 1992). At the N-terminus of the peptide, where hydrogen bond formation does not contribute to the base-catalyzed exchange kinetics, the magnitude of the rate enhancement corresponds to a free energy of 0.2–0.4 kcal mol^{-1}, in reasonable agreement with previous measurements of the helix macrodipole potential in isolated peptide helices (Lockhart & Kim, 1993; Huyghues-Despointes et al., 1993; Armstrong & Baldwin, 1993).

The macrodipole potential is also expected to affect the exchange kinetics measured at the C-terminus of the peptide. For two C-terminal alanine peptide units that cannot form CO hydrogen bonds, no shift in pH_{min} is expected in the absence of electrostatic effects (see above), but the negative electrostatic potential of the helix macrodipole should increase the acid-catalyzed rate and decrease the base-catalyzed rate, increasing pH_{min}. Significant increases in the pH_{min}, however, are not observed for C-terminal amides (Table 1), suggesting that

this additional contribution to the exchange kinetics is specific to N-terminus of the peptide. This observation indicates that explanations for the observed rate enhancement of base-catalyzed exchange that do not rely on the helix macrodipole should be considered. One possibility is that the pK_a values of the peptide nitrogens are decreased at the N-terminus of the peptide as a result of electron-withdrawing CO hydrogen bonds formed by these peptide groups. Increased acidity of the peptide NH would result in increased rates of base-catalyzed exchange. Alternatively, the N-terminal peptide NHs may have increased solvent accessibility in the helical peptide relative to the corresponding amide protons in the nonhelical reference peptide. Increased solvent accessibility of the nonbonded NHs should affect only the kinetics of base-catalyzed exchange at the N-terminus of the peptide, accounting for the asymmetry of the effect. Because the helix macrodipole is screened by salt (Scholtz et al., 1991b; Lockhart & Kim, 1993; Huyghues-Despointes et al., 1993), it should be possible to distinguish between an electrostatic contribution to exchange from the helix macrodipole and alternative models by observing the salt dependence of the exchange kinetics.

Interpretation of Amide Proton Exchange in α-Helices by Modified Lifson–Roig Theory. In predicting protection factors for exchange from the helical peptide, hydrogen bonding and the accompanying decrease in solvent accessibility were considered to be the dominant factors affecting the observed exchange kinetics. In our model, the protection factor for base-catalyzed exchange is directly related to the extent of hydrogen bonding of the peptide NH. Because acid-catalyzed exchange occurs by O-protonation, the protection factor depends on the extent of hydrogen bonding of both the NH and CO groups of a peptide unit. The predicted protection factors are in reasonable agreement with the experimental values (Figure 3). In the peptide center, nearly all the predicted protection factors are slightly smaller than the measured values. This difference may reflect some residual structure in the open conformation. Once the required hydrogen bonds have been broken, peptide groups may still have restricted access to solvent, thus reducing their exchange rates relative to the unstructured reference peptide.

In our earlier interpretation of total NH exchange kinetics for a series of repeating-sequence alanine-based peptides of differing chain lengths (Rohl et al., 1992), the kinetic data fit a model that correlates protection only with hydrogen bonding of peptide NH groups, despite the fact that the kinetics were measured at pH* 2.5, where exchange occurs predominantly by the acid-catalyzed mechanism. Because the helix-coil transition is cooperative, states in which both the NH and CO hydrogen bond of a peptide unit are either broken or formed are much more common than those in which one hydrogen bond is formed and the other is not. Consequently, the mechanism in which protection from exchange results from two hydrogen bonds predicts protection factors of roughly the same magnitude as the mechanism in which only one hydrogen bond provides protection. Total NH exchange, which only measures the magnitude of protection, cannot distinguish between these two mechanisms. Individual protection factors provide a more detailed picture of the hydrogen bonding network in the helix and allow the mechanisms of acid- and base-catalyzed exchange to be tested. Amide proton exchange measurements provide both site-specific and quantitative characterization of helix stability. Although isolated peptide helices are not very stable in aqueous solution, the hydrogen-bonded amide protons are measurably protected from exchange. The amide exchange method shows great potential as a tool for studying helix formation in isolated peptides and should be useful for studying helical side chain and capping interactions.

ACKNOWLEDGMENT

We thank Drs. Stewart Loh and Andrew Doig for critical review of the manuscript and Dr. Hong Qian for helpful discussions of helix-coil theory. The computer program implementing the Lifson–Roig helix-coil theory was originally written by Dr. John Schellman and modified by Dr. Hong Qian. Further modifications to include capping interactions were added by C.A.R. We thank the Mass Spectrometry Facility, University of San Francisco, supported by NIH Grant RR 01614, for FAB mass spectra and the Protein and Nucleic Acid Facility, Stanford University, for electrospray mass spectra.

REFERENCES

Armstrong, K. M., & Baldwin, R. L. (1993) *Proc. Natl. Acad. Sci. U.S.A. 90*, 11337–11340.
Atherton, E., & Sheppard R. C. (1989) *Solid Phase Peptide Synthesis: A Practical Approach*, IRL Press, New York.
Bai, Y., Milne, J. S., Mayne, L., & Englander, S. W. (1993) *Proteins: Struct., Funct., Genet. 17*, 75–86.
Bendall, M. R., Pegg, D. T., Doddrell, D. M., & Field, J. (1981) *J. Am. Chem. Soc. 103*, 934–936.
Bradley, E. K., Thomason, J. F., Cohen, F. E., Kosen, P. A., & Kuntz, I. D. (1990) *J. Mol. Biol. 215*, 607–622.
Chakrabartty, A., & Baldwin, R. L. (1994) *Adv. Protein Chem.* (submitted).
Chakrabartty, A., Schellman, J. A., & Baldwin, R. L. (1991) *Nature 351*, 586–588.
Chakrabartty, A., Kortemme, T., & Baldwin, R. L. (1994) *Protein Sci. 3*, 843–852.
Covington, A. K., Robinson, R. A., & Bates, R. G. (1966) *J. Phys. Chem. 70*, 3820–3824.
Dempsey, C. E. (1986) *Biochemistry 25*, 2904–3911.
Dempsey, C. E. (1988) *Biochemistry 27*, 6893–6901.
Dempsey, C. E. (1992) *Biochemistry 31*, 4705–4712.
Doig, A. J., Chakrabartty, A., Klingler, T. M., & Baldwin, R. L. (1994) *Biochemistry 33*, 3396–3403.
Englander, S. W., & Kallenbach, N. R. (1984) *Q. Rev. Biophys. 16*, 521–655.
Fiori, W. R., Miick, S. M., & Millhauser, G. L. (1993) *Biochemistry 32*, 11957–11962.
Freeman, R., Mareci, T. H., & Morris, G. A. (1981) *J. Magn. Reson. 42*, 341–345.
Gans, P. J., Lyu, P. C., Manning, M. C., Woody, R. W., & Kallenbach, N. R. (1991) *Biopolymers 31*, 1605–1614.
Gregory, R. B., Crabo, L., Percy, A. J., & Rosenberg, A. (1983) *Biochemistry 22*, 910–917.
Hudson, D. (1988) *J. Org. Chem. 53*, 617–624.
Huyghues-Despointes, B. M. P., Scholtz, J. M., & Baldwin, R. L. (1993) *Protein Sci. 2*, 1604–1611.
Hvidt, A. (1964) *C. R. Trav. Lab. Carlsberg 34*, 299–317.
Jimenez, M. A., Blanco, F. J., Rico, M., Santoro, J., Herranz, J., & Nieto, J. L. (1992) *Eur. J. Biochem. 207*, 39–49.
Kuwajima, K., & Baldwin, R. L. (1983) *J. Mol. Biol. 169*, 299–323.
Liff, M. I., Lyu, P. C., & Kallenbach, N. R. (1991) *J. Am. Chem. Soc. 113*, 1014–1019.
Lifson, S., & Roig, A. (1961) *J. Chem. Phys. 34*, 1963–1974.
Linderstrøm-Lang, K. (1955) *Chem. Soc. Spec. Publ. No. 2*, 1–20.
Lockhart, D. J., & Kim, P. S. (1993) *Science 260*, 198–202.
Lyu, P. C., Liff, M. I., Marky, L. A., & Kallenbach, N. R. (1990) *Science 250*, 669–673.
Marqusee, S., Robbins, V. H., & Baldwin, R. L. (1989) *Proc. Natl. Acad. Sci. U.S.A. 86*, 5286–5290.

Miick, S. M., Todd, A. P., & Millhauser, G. L. (1991) *Biochemistry 30,* 9498–9503.
Miick, S. M., Martinez, G. V., Fiori, W. R., Todd, A. P., & Millhauser, G. L. (1992) *Nature 359,* 653–655.
Miick, S. M., Casteel, K. M., & Millhauser, G. L. (1993) *Biochemistry 32,* 8014–8021.
Molday, R. S., Englander, S. W., & Kallen, R. G. (1972) *Biochemistry 11,* 150–158.
Nakanishi, M., Tsuboi, M., Ikegami, A., & Kanehisa, M. (1972) *J. Mol. Biol. 64,* 363–378.
Osterhout, J. J., Baldwin, R. L., York, E. J., Stewart, J. M., Dyson, H. J., & Wright, P. E. (1989) *Biochemistry 28,* 7059–7064.
Pease, J. H. V., Storrs R. W., & Wemmer, D. E. (1990) *Proc. Natl. Acad. Sci. U.S.A. 87,* 5643–5647.
Perrin, C. L. (1989) *Acc. Chem. Res. 22,* 268–275.
Perrin, C. L., & Arrhenius, G. M. L. (1982) *J. Am. Chem. Soc. 104,* 6693–6696.
Perrin, C. L., Loll, C. P., & Johnston, E. R. (1984) *J. Am. Chem. Soc. 106,* 2749–2753.
Ptitsyn, O. B. (1972) *Pure Appl. Chem. 31,* 227–244.
Radford, S. E., Dobson, C. M., & Evans, P. A. (1992) *Nature 358,* 302–207.
Robertson, A. D., & Baldwin, R. L. (1991) *Biochemistry 30,* 9907–9914.
Roder, H., Wagner, G., & Wüthrich, K. (1985) *Biochemistry 24,* 7407–7411.
Rohl, C. A., Scholtz, J. M., York, E. J., Stewart, J. S., & Baldwin, R. L. (1992) *Biochemistry 31,* 1263–1269.
Scholtz, J. M., & Baldwin, R. L. (1992) *Annu. Rev. Biophys. Biomol. Struct. 21,* 95–118.
Scholtz, J. M., Qian, H., Robbins, V. H., & Baldwin, R. L. (1993) *Biochemistry 32,* 9668–9676.
Scholtz, J. M., York, E. J., Stewart, J. M., & Baldwin, R. L. (1991b) *J. Am. Chem. Soc. 113,* 5102–5104.
Scholtz, J. M., Qian, H., York, E. J., Stewart, J. M., & Baldwin, R. L. (1991a) *Biopolymers 31,* 1463–1470.
Shaka, A. J., Keeler, J., Frenkiel, T., & Freeman, R. (1983) *J. Magn. Reson. 53,* 335–338.
Stewart, J. M., & Young, J. D. (1984) *Solid Phase Peptide Synthesis,* Pierce Chemical Co., Rockland, IL.
Tüchsen, E., & Woodward, C. (1985) *J. Mol. Biol. 185,* 421–430.
Wand, A. J., Roder, H., & Englander, S. W. (1986) *Biochemistry 25,* 1107–1114.
Woodward, C., Simon, I., & Tüchsen, E. (1982) *Mol. Cell. Biochem. 48,* 135–160.
Zhou, H. X., Hull, L. A., Kallenbach, N. R., Mayne, L., Bai, Y., & Englander, S. W. (1994) *Proteins: Struct., Funct., Genet.* (submitted).
Zimm, B. H., & Bragg, J. K. (1959) *J. Chem. Phys. 31,* 526–535.